Swelling behaviour of quartz crystal microbalance sensors coated with graphene Langmuir-Blodgett films

Y. ACIKBAS*
Department of Materials Science and Nanotechnology Engineering, Faculty of Engineering, University of Usak, Turkey

This study reports the characterization and gas sensing applications of graphene by using UV-visible spectroscopy, Quartz Crystal Microbalance (QCM) and Langmuir-Blodgett (LB) thin film deposition techniques. The graphene LB thin films are characterized by using UV-visible spectroscopy and QCM system. The transfer ratio values are found to be over 0.95 for quartz glass or quartz crystal substrates. The typical frequency shift per layer is obtained as 53.65 Hz/layer and the deposited mass onto quartz crystal is calculated as 988.02 ng/layer. The swelling behaviours of the graphene LB films are also investigated with respect to volatile organic compounds (VOCs) at room temperature by using the early-time Fick's law of diffusion. It is observed that the diffusion coefficients (D) for swelling obeyed the $t^{1/2}$ law and are correlated with the VOCs used. The diffusion coefficients are found to be 29.18 x 10^{-16}, 21.76 x 10^{-16}, 2.10 x 10^{-16} and 1.49 x 10^{-16} cm^2 s^{-1} for dichloromethane, chloroform, benzene and carbontetrachloride, respectively. The response of the graphene films to the selected VOCs has been investigated in the conditions of the physical properties of the solvents, and the films are obtained to be largely sensitive to dichloromethane and chloroform vapors compared to the other studied vapors.

(Received January 07, 2016; accepted April 05, 2016)

Keywords: Graphene, Diffusion coefficient, Swelling, Quartz Crystal Microbalance (QCM), Langmuir-Blodgett (LB) Thin films, Sensors

1. Introduction

Graphene, a single atomic layer of carbon, has attracted considerable attention due to its important physical properties, such as high carrier mobility and conductivity, high transparency, mechanical flexibility and environmental stability [1,2]. It has attracted great attention and shown to have great potential for applications of fabricating electronic devices, photovoltaic devices, fuel cells, nanocomposites, sensors and nanocarriers [3-6]. The sensors using graphene materials have been attracted due to its excellent conductivity, a large surface area and strong mechanical strength [7]. Zhihua and co-workers have developed a sensor based on quartz crystals coated with a thin layer of graphene to detect formaldehyde (HCHO). The graphene sensor displays certain frequency changes when exposed to various concentrations of HCHO. The results indicate that a graphene modified QCM exhibits great potential for trace detection of HCHO with perfect linear correlation [8]. A similar study was carried out by Quang et al. [9] to investigate the gas-sensing properties of the graphene-coated QCM sensor at the room temperature. The researchers have demonstrated that the graphene-coated QCM sensor can be used in a VOC sensing application and the sensor showed the highest sensitivity with ethanol among the VOCs used in that work. QCM ammonia sensor have been developed to investigate the quality (Q) factor of the QCMs which was measured with and without the graphene oxide (GO) isolation layer between the electrode of the QCM and polyaniline (PANI) sensing film. The experimental results demonstrated that the introduction of GO isolation layer can effectively improve the Q factor of the QCM [10].

The most important process in VOCs identification is the preparation of the thin film sensors. There are several methods for thin film fabrication such as casting, spin coating, chemical or physical vapor deposition, and Langmuir-Blodgett (LB) thin film technique. Using LB technique, compared with the other coating methods, it is possible to prepare a thin film with a controlled thickness at the molecular level with a well-defined molecular orientation [11]. This technique offers an effective way to prepare well-defined structure of graphene LB film [12], which is promising for chemical sensors device applications [13].

To the best of our knowledge, there is no work in the literature that investigates VOCs swelling behaviours of graphene molecule based on mass change using the early-time Fick's law of diffusion. In this work, the graphene was selected as potential sensor material to investigate the swelling behaviours of the graphene LB thin film using QCM technique. To study the swelling mechanism in sensor applications, LB films were subjected to the saturated VOCs vapors. The frequency shift of the quartz resanators was recorded as a function of time during swelling resulted from the bulk diffusion process. The calculated diffusion coefficients (D) of VOCs by using Early-time Fick's law of diffusion was adopted to fit the QCM results.

2. Experimental details

Graphene used in thin film fabrication was purchased from Sigma Aldrich. The chemical structure of the graphene has been given in the Fig.1. The selected organic vapor molecules were dichloromethane, chloroform, benzene and carbontetrachloride because of their toxicity and harmful effects on human health. All were purchased from Sigma Aldrich.

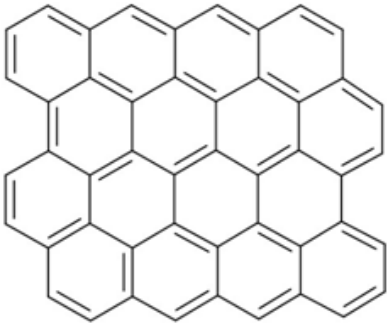

Fig. 1. The chemical structure of graphene.

Graphene material could be dissolved in dimethylformamide (DMF) with a ratio of concentration approximately 0.23 mg ml^{-1}. This solution was used to take an isotherm and to produce LB film by spreading it on the distilled water surface. Before the isotherm graph was taken, 15 minutes was allowed for the solvent to evaporate. The isotherms were recorded with the compression speed of 30 cm^2 min^{-1} at pH 6.0. The isotherm graph was repeated several times and the results were found to be reproducible at the room temperature. In this study, the deposition pressure and deposition mode were 18 mN m^{-1} and Z-type, respectively.

The Fig. 2 shows a block diagram of our homemade QCM measurement system. A thinly cut wafer of raw quartz sandwiched between two electrodes in an overlapping keyhole design was used for the QCM measurement. AT-cut quartz crystals with a resonant frequency of 3.5 MHz were commercialized from GTE SYLVANIA company. All measurements were taken at the room temperature (20 ^oC) using an oscillating circuit designed in-house. At the beginning of the measurement, a clean quartz crystal was inserted into the electronic unit, and the quartz crystal was placed in a gas chamber. In order to obtain f_0, which is the resonant frequency of non-coated quartz crystal, the frequency shift of quartz crystal was measured, and the frequency response was stable within ±1 Hz over a period of 30-45 minutes. After each deposition cycle, the LB film sample was dried for half an hour and the mass change was monitored using the computer controlled QCM measurement system. The system was used for the confirmation of the reproducibility of LB film multilayers using the relationship between the QCM frequency changes against the deposited mass, which should depend on the number of layers in the LB film.

A gas cell was constructed to study the LB film response on exposure to organic vapors by measuring the frequency change and these measurements were performed with a syringe. The sample was periodically exposed to organic vapors at least for two minutes, and was then allowed to recover after injection of dry air. The changes in the resonance frequency were recorded in real time during exposure to organic vapors. This procedure was carried out over several cycles to observe the reproducibility of the LB film sensing element.

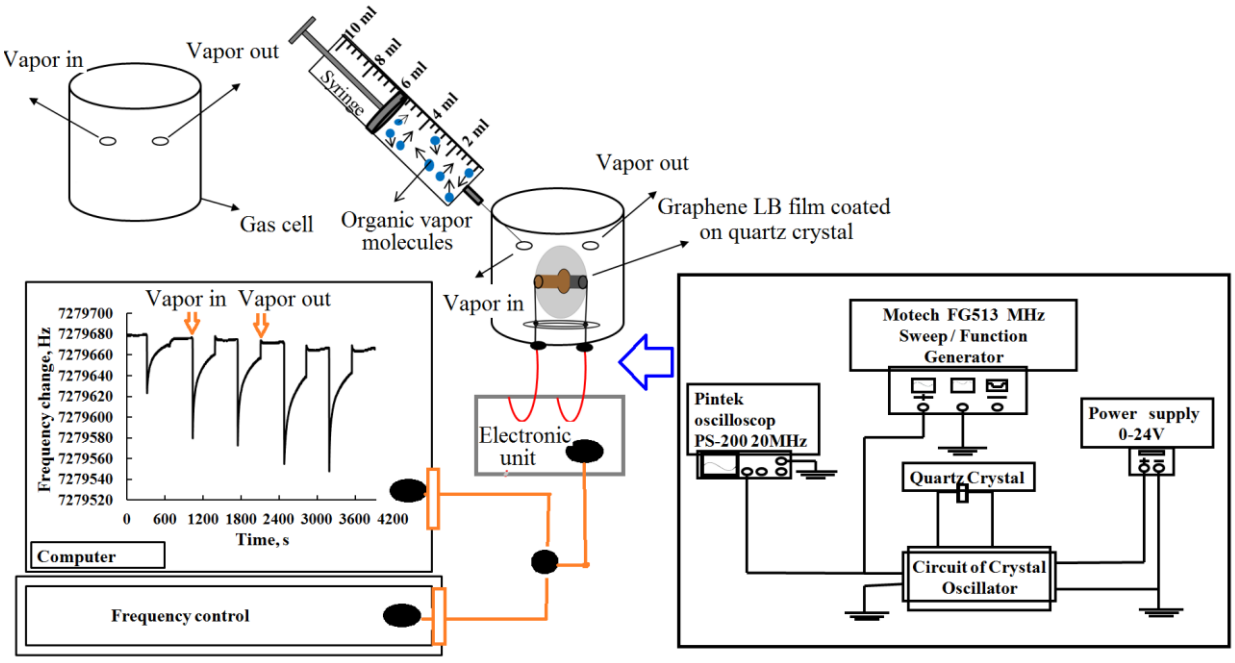

Fig. 2. A block diagram of the quartz crystal microbalance measurement system.

3. Result and discussion

3.1. Isotherm properties and transfer ratio

The Fig. 3 shows the isotherm graph (π-A) of the graphene with the different amount of graphene solution being applied. The first inflection point of π-A isotherms shifted to the larger area side with increasing amount of solution from 400 µl to 1800 µl. This tendency reflected the positive relationship between the number of graphene molecules stable at the air/water interface and the amount of solution being scattered. When there is a little interaction between the molecules, the surface pressure is unchanged or nearly zero as given plot for 400 µl. If the barrier is compressed very slowly and the confirmed area is reduced, the graphene molecules are forced closer together and the surface pressure begins to increase. A similar study was carried out by Jia and Zou using sulphonated graphene nanosheets (GNSs) solution to obtain an ideal π-A isotherm graph [14].

The suitable surface pressure for graphene LB film deposition procedure was selected as 18 mN m^{-1}. The transfer ratio for a Langmuir-Blodgett thin film deposition is also an important parameter to monitor the deposition process. It is defined as the ratio of the area of the Langmuir-Blodgett film removed from the water surface to the area of the substrate moved through the air-monolayer-water surface.

$$TR = A_1 / A_2 \tag{1}$$

where A_1 is the occupied area by the monolayer on the water surface, and A_2 is the deposited area of the quartz crystal or quartz glass substrate. The reduced surface area change of the graphene monolayers during the deposition onto a quartz glass substrate for 5 bilayers is given the inset of the Fig. 3. The labels of the inset in the Fig. 3 are pointed from position (a) to position (b) right-to-left direction when the first LB film layer deposited onto the quartz glass substrate. A similar labelling is made for the second, third, fourth and fifth layers. It is found that the average reduction of the area for each bilayer was almost the same during the deposition process of monolayers onto the quartz glass substrate. The tranfer ratio values are calculated using the Eq. 1, and these values are obtained to be over 0.95 for graphene molecules. Those results indicate that graphene molecules can be successfuly deposited onto solid substrates with remarkable transer ratios.

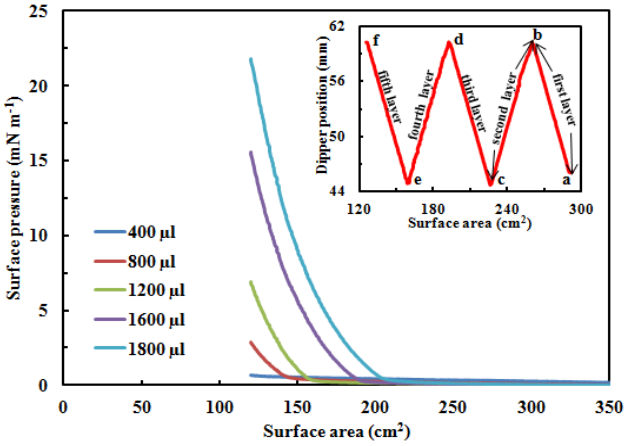

Fig. 3. Isotherm graph of the graphene monolayer. Inset: The number of LB deposition cycles of the graphene thin film onto quartz glass substrate.

3.2. QCM and UV-visible measurements

QCM system is fairly sensitive to small mass changes at nanoscale which is used for measuring the resonance frequency of quartz crystal. The resonance frequency change (Δf) on LB film multilayer quartz crystal against a mass change per unit area (Δm) is given by [15]:

$$\Delta f = -\left(2 f_0^2 \Delta m / \rho_q^{1/2} \mu_q^{1/2} A\right) N \tag{2}$$

where, Δf is the frequency change (Hz), f_0 is the resonant frequency of non-coated quartz crystal (Hz), Δm is the deposited mass per unit area per layer (g), ρ_q is the density of quartz (2.648 g cm^{-3}), μ_q is the shear modulus of quartz (2.947x 10^{11} g cm^{-1} s^{-2}), A is the electrode active area (2.65 cm^2) and N is the number of deposited LB film layers.

The Fig. 4 describes the deposition of the graphene LB films onto quartz resonators for ten layers. The change in the resonance frequency as a function of the number of monolayers is closely associated with the LB layer mass change. A linear dependence reveals that equal amount of mass per unit area is deposited onto the quartz crystal during the deposition of LB film layers. The frequency shifts of 53.65 Hz / per layer for the graphene LB films are obtained from the curve of the plot. The mass deposited on the quartz crystal per bilayer is estimated as 988.02 ng (3.72 ng mm^{-2}) for the graphene LB film using the Eq. 2 and Fig. 4.

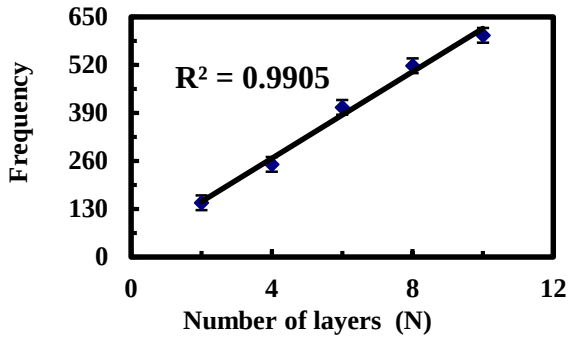

Fig. 4. Frequency changes as a function of graphene LB film layer numbers.

The Fig. 5 displays both the UV-vis absorption spectra of graphene solution in DMF and graphene LB films transferred onto a quartz glass substrate with different layer thicknesses. The UV-vis spectrum of the graphene solution is observed at around 250 nm. The Fig. 5 also shows the absorption spectra at 220 nm for two to ten layers of the graphene LB films on the quartz glass substrate. The UV-vis spectra of the LB films are similar to the solution spectra but the band at 220 nm is broadened in the solution spectrum and is blue shifted by about 30 nm. The shift in the absorption band of the LB film may be the result of some kind of molecular aggregation occured during film formation. In order to monitor the deposition of LB film layer onto the quartz substrate, the relationship between the absorbance and layer numbers is investigated. The inset in the Fig. 5 shows a plot of the absorption intensity at 220 nm relative to the layer numbers of LB films which demonstrates an almost linear increase of the absorption intensity with the layer numbers. The linear relationship between the absorbance and the number of layers suggests that a regular deposition of the graphene monolayer takes place, resulting in fairly uniform LB films. This means that similar amount of the graphene is transferred during each LB deposition. Similar linear relationships were obtained with plots of the absorbance for graphene and gold nanoparticles LB film layers by Shakir et al. [16].

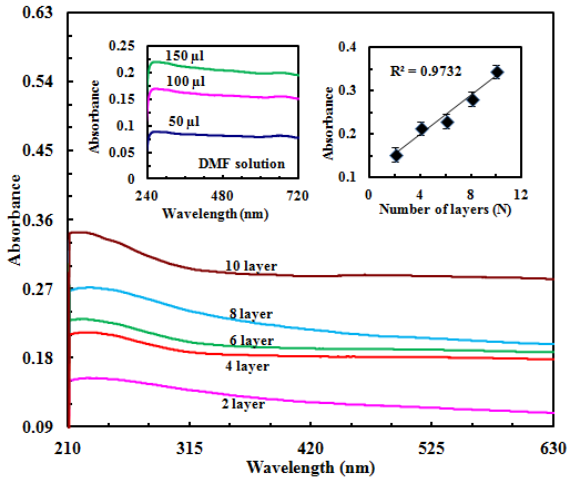

Fig. 5. UV-vis spectras of the graphene in a chloroform solution and the graphene LB film on the quartz glass. Inset: linear increase of absorbance as a function of layer numbers.

3.3 Sensing properties of the graphene LB film

The Fig. 6 shows the kinetic response for ten layers the graphene LB films against to the saturated organic vapors. In the Fig. 6, the frequency shift was monitored as a function of time during periodic exposure of the graphene LB film sensor to several organic vapors (dichloromethane, chloroform, benzene and carbontetrachloride) for two minutes, followed by the injection of dry air for another two minutes period. The inset in the Fig. 6 displays the reproducibility of the graphene LB thin film for dichloromethane vapor. The graphene sensing film was found to be stable and exhibited no significant losses in sensitivity when the measurements were repeated many times.

In the initial step, the graphene LB film sensor was exposed to fresh air for 120 s, and a stable value was obtained as a response. In the second step, the first response of Langmuir-Blodgett film sensor to organic vapors was carried out between 120 and 125 s because of the surface adsorption effect between Langmuir-Blodgett film sensor and organic vapors. After this interaction, the bulk diffusion process caused an increase in effective mass, which reduces the response of the Langmuir-Blodgett film sensor, in direct proportion to the VOCs pressure. The frequency shifted as function of the number of adsorbed VOC molecules. In the third step (in the 240 s), after the fresh air was injected by syringe into the sensing chamber, the gas molecules adsorbed to the surface of the thin film were quickly separated from the surface. Therefore, a rapid decrease on sensor response occurred between 240 and 244 s while the adsorption continued. In the last step, after 245 s, the response of thin film sensor attained an initial baseline. QCM kinetic measurement was carried out for three cycles to observe reproducibility of sensor material. These three cycles of kinetic measurement indicated that the sensor response is reproducible for all organic vapors used in this study.

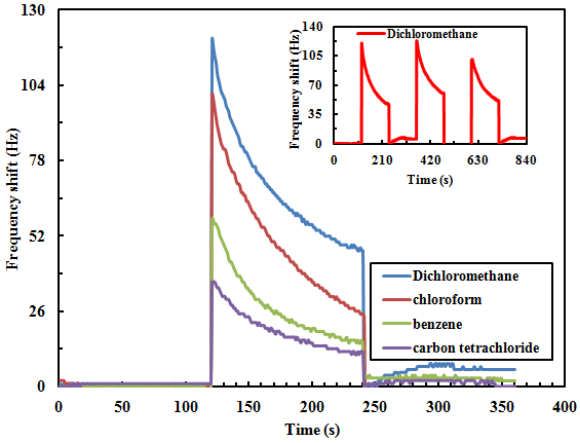

Fig. 6. The frequency change of the graphene LB film against organic vapors.

When Fick's second law of diffusion is applied to a plane sheet and solved by assuming a constant diffusion coefficient, the following equation is obtained for concentration changes in time [17]:

$$\frac{C}{C_0} = \frac{x}{d} + \frac{2}{\pi}\sum_{n=1}^{\infty}\frac{\cos n\pi}{n}\sin\frac{n\pi x}{d}\exp(-\frac{Dn^2\pi^2}{d^2}t) \quad (3)$$

where d is the thickness of the slab, D is the diffusion coefficient, and C_0 and C are the concentration of the diffusant at time zero and t, respectively. x corresponds to the distance at which C is measured. We can replace the concentration terms directly with the amount of diffusant by using:

$$M = \int_V C dV \quad (4)$$

where M is the mass uptake and V is the volume element. When the Eq. 1 is considered for a plane volume element and substituted into the Eq. 4, the following solution is obtained [18].

$$\frac{M_t}{M_\infty} = 1 - \frac{8}{\pi^2}\sum_{n=0}^{\infty}\frac{1}{(2n+1)^2}\exp(-\frac{(2n+1)^2 D\pi^2}{d^2}t) \quad (5)$$

where M_t penetrant mass sorbed into the deposited film, assuming a one-dimensional geometry. The quantity, M_∞, represents the amount sorbed at equilibrium, t is the time. This equation can be reduced to a simplified form:

$$\frac{M_t}{M_\infty} = 4\sqrt{\frac{D}{\pi d^2}}t^{1/2} \quad (6)$$

which is called early-time equation and this square root relation can be used to interpret the swelling data [19].

To measure the kinetic data given in the Fig. 6, it is required to take the graphene LB film parameters because of swelling. The Fig. 7 represents the normalized frequency change against swelling time where the consolidation process involves setting starting times to $t = 0$ for each swelling cycles. It can be seen that the changes in the normalized frequency against the time of vapor exposure decreased very fast as the saturated vapor injected into the gas cell is increased. These behaviours can be declared with the chain inter diffusion between graphene chains during vapor exposure. As the saturated vapors penetrate into graphene film, the graphene chains interdiffuse, which results in the decrease of the normalized frequency from the graphene film. These results can be related to the amount of diffusant entering into the graphene film M_t; that is, Δ_{ft} should be directly proportional to M_t [17]. The Eq. 6 now can be written as:

$$\left(\frac{M_t}{M_\infty}\right) \approx \left(\frac{\Delta f_t}{\Delta f_\infty}\right) = 4\sqrt{\frac{D}{\pi d^2}}t^{1/2} \quad (7)$$

where Δ_{ft} and $\Delta_{f\infty}$ are the normalized frequency shift at any time, t and saturation point in Δ_f, respectively. The normalized Δ_f values [$\Delta_{ft}/\Delta_{f\infty}$] are plotted in the Fig. 8 for the square root of swelling time according to the Eq. 7. The slopes of the linear relations in the Fig. 8 indicate the diffusion coefficients, D_s for the swelling of graphene film.

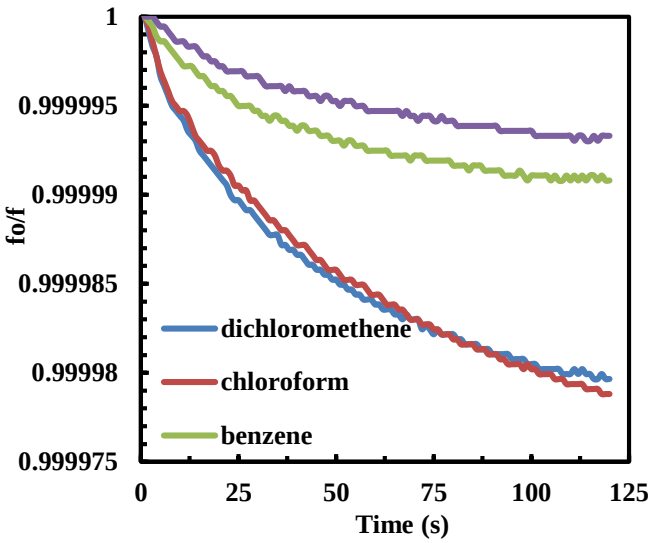

Fig. 7. Normalized frequency changes against swelling time, t_s for organic vapors

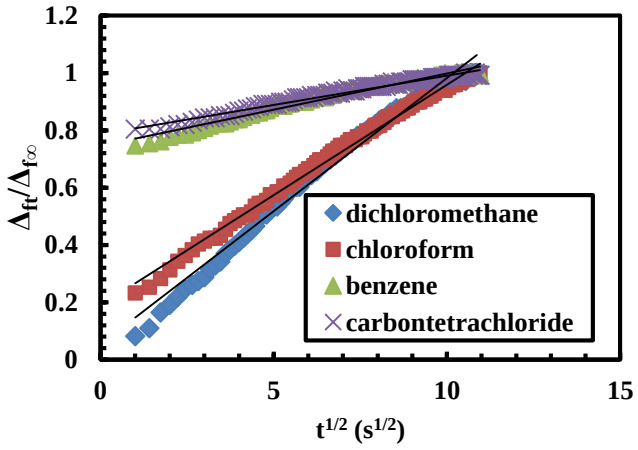

Fig. 8. Plot of the normalized frequency against square root of swelling time, t_s. The solid line represents the fit of the data to the Eq. 7.

As shown in the Fig. 6, the resonance frequency changes of the graphene thin film sensor for the organic vapors are, apparently, in the following order: dichloromethane > chloroform > benzene > carbontetrachloride. A similar result was found for diffusion coefficients as 29.18 x 10^{-16}, 21.76 x 10^{-16}, 2.10 x 10^{-16} and 1.49 x 10^{-16} cm^2 s^{-1} for organic vapors, respectively. The interaction of these gases with the LB thin films is believed to be a physical absorption through a dipole/dipole interaction or hydrogen bonding [20]. The high values of diffusion coefficient obtained for chlorinated aliphatic hydrocarbons especially for dichloromethane and chloroform were comparable with other organic vapors. This may be explained by the high dipole moment values of dichloromethane (1.60 D) and chloroform (1.04 D) which explains this effect as previously been reported by other research groups [21,22]. Relatively lower responses were observed for carbontetrachloride (0 D) and benzene (0 D). However, the sensitivity of the graphene film sensor against

carbontetrachloride vapor is slower than the other vapors used in this work. This can be clarified with the fact that the molar volume of carbontetrachloride is larger than the dichloromethane, chloroform and benzene (can be seen in the Table 1). While carbontetrachloride molecule can have difficulty to diffuse into the graphene thin films, the penetration of other vapor molecules into the same thin films is faster.

Table 1. The physical properties of the VOCs.

	Molar volume	Dipol moment	Diffusion coefficients
Organic vapors	(cm^3 mol^{-1})	(D)	Ds (cm^2 s^{-1})x10^{-16}
Dichloromethane	64.10	1.60	29.18
Chloroform	80.70	1.08	21.76
Benzene	86.36	0	2.10
Carbontetrachloride	97.10	0	1.49

4. Conclusion

In this study, the graphene was characterized and investigated for its gas sensing properties using Langmuir-Blodgett (LB), UV-vis spectroscopy and QCM techniques. Graphene LB film transfer on the solid substrate has been found to be successful with a high transfer ratio of ~ 0.95. Also, a linear relationship between the number of layers and the absorbance shift indicated that the graphene molecules are deposited orderly onto solid substrates. A similar linear relationship was obtained with respect to deposited mass onto quartz crystal substrate, which was observed for resonant frequencies versus layer number. The typical Δf per layer was 53.65 Hz / layer and the deposited mass onto quartz crystal was calculated as 988.02 ng / layer (3.72 ng mm^{-2}). The diffusion coefficients were found to be 29.18 x 10^{-16}, 21.76 x 10^{-16}, 2.10 x 10^{-16} and 1.49 x 10^{-16} cm^2 s^{-1} for dichloromethane, chloroform, benzene and carbontetrachloride, respectively. The QCM results showed that the response to chlorinated aliphatic hydrocarbons (dichloromethane and chloroform vapors) is higher than that of the other organic vapors used in this work. Those results could be clarified with the dipole moment and molar volume of organic vapors. The response has been attributed to dipole/dipole interaction or hydrogen bonding between the thin films and the gas molecules. The graphene material can be used as a sensing material and may find potential applications in the development of room temperature organic vapor sensing devices.

Acknowledgements

The author would like to thank The Research Foundation of Usak University (BAP and UBATAM) for financial support of this work. Project no.: 2014/MF014. Thank you very much to Dr. Rifat Capan and Dr. Matem Erdogan for their help.

References

[1] W. Cai, S. Jiang, S. Xu, Y.Li, J.Liu, C. Li, L. Zheng, L. Su, J. Xu, Opt. Laser Techon. **65,** 1 (2015).
[2] Y. Zhang, L. Du, Y. Lei, H. Zhao, Mater. Lett. **131,** 288 (2014).
[3] Z. Zhu, Min Su, L. Ma, L. Ma, D. Liu, Z. Wang, Talanta **117,** 449 (2013).
[4] H. Zhang, G. Grüner, Y. Zhao, J. Mater. Chem. B **1,** 2542 (2013).
[5] Q. Liu, Z. F. Liu, X. Y. Zhang, N. Zhang, L. Y. Yang, S. G. Yin, Y. S. Chen, Appl. Phys. Lett. **92**, 223303 (2008).
[6] B. Seger, P. V. Kamat, J. Phys. Chem. C **113**, 7990 (2009).
[7]Y. Yao, X. Chen, H. Guo, Z. Wu, Appl. Surf. Sci. **257,** 7778 (2011).
[8] Y. Zhihua, Z. Liang, S. Kaixin, H. Weiwei, Procedia Eng. **29,** 2448 (2012).
[9] V.V. Quang, V.N. Hung, L.A. Tuan, V.N. Phan, T. Q. Huy, N.V. Quy, Thin Solid Films **568,** 6 (2014).
[10] X. Li, X. Chen, Y. Yao, N. Li, X. Chen, Sens. Actuators B: Chem. **196,** 183 (2014).
[11] I. Capan, C. Tarımcı, R. Capan, Sens. Actuators B: Chem. **144,** 126 (2010).
[12] V.D. Botcha, P.K. Narayanam, G. Singh, S.S. Talwar, R.S. Srinivasa, S.S. Major, Colloids Surf. A Physicochem. Eng. Asp. **452**, 65 (2014).
[13] Y. Yao, X. Chen, X. Li, X. Chen, N. Li, Sens. Actuators B: Chem. **191**, 779 (2014).
[14] B. Jia, L. Zou, Chem. Phys. Lett. **568-569**, 101 (2013).
[15] Y. Acikbas, R. Capan, M. Erdogan, F. Yukruk, Res. Eng. Struct. Mat. **2,** 99 (2015).
[16]. I. Shakir, Z. Ali, D. J. Kang, Journal of Alloys and Compounds **617**, 707 (2014).
[17] M. Erdogan, R. Capan, F. Davis, Sens. Actuators B: Chem. **145**, 66 (2010).
[18] J. Crank, The Mathematics of Diffusion, Oxford University Press, London (1970).
[19] M. Erdogan, I. Capan, C. Tarimci, A.K. Hassan, J. Colloid Interf. Sci. **323**, 235 (2008).
[20] İ. Çapan, B. İlhan, J. Optoelectron. Adv. Mater. **17**, 456 (2015).
[21] S. Ichinohe, H. Tanaka, and Y. Kanno, Sens. Actuators B: Chem. **123**, 306 (2007).
[22] T. Ceyhan, A. Altındal, A.R. Özkaya, M.K. Erbil, Ö. Bekaroğlu, Polyhedron **26**,73 (2007).

*Corresponding author: yaser.acikbas@usak.edu.tr